

# Reconstructing Historical Solar Activity with the Advective Flux Transport Model

Our Window Into The TSI of the Past

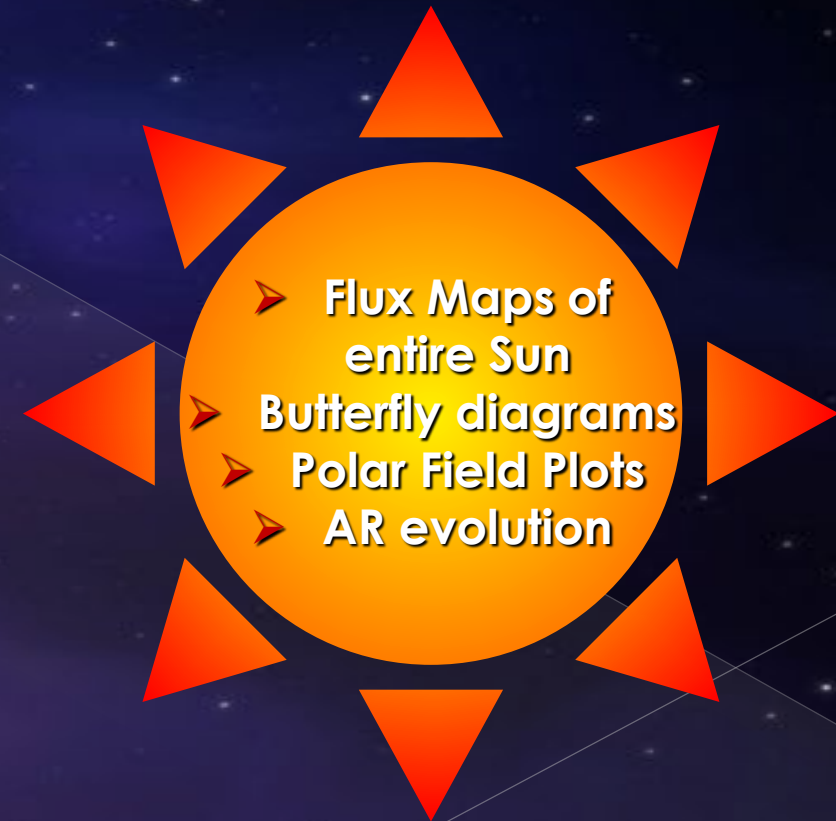
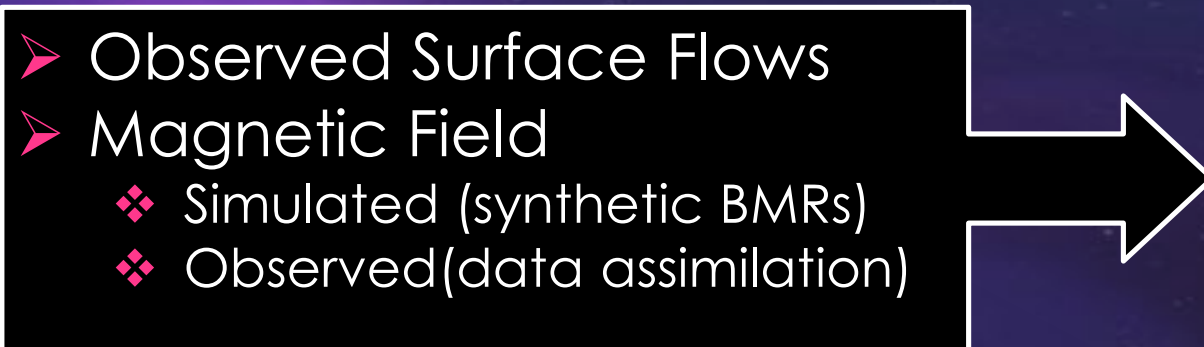
Lisa Upton, Greg Kopp, Odele Coddington, and Judith Lean

# Introduction

- ◉ Surface flux transport (SFT) models simulate the evolution of the photospheric magnetic field.
- ◉ We are working on a project to create an updated historical TSI reconstruction based on the new SSN.
  - > SSN -> SFT -> Open and Closed Flux -> TSI Models
- ◉ This talk will focus on the SSN -> SFT -> Flux
  - > (go see Greg's Poster for more info on the TSI modeling)
- ◉ Wang, Lean, and Sheeley (2000-2005)

# The Advective Flux Transport Model

Upton & Hathaway have developed a state of the art SFT model, the Advective Flux Transport (AFT) model. This advanced model advects the surface field with the observed flows, reproducing magnetic field evolution.



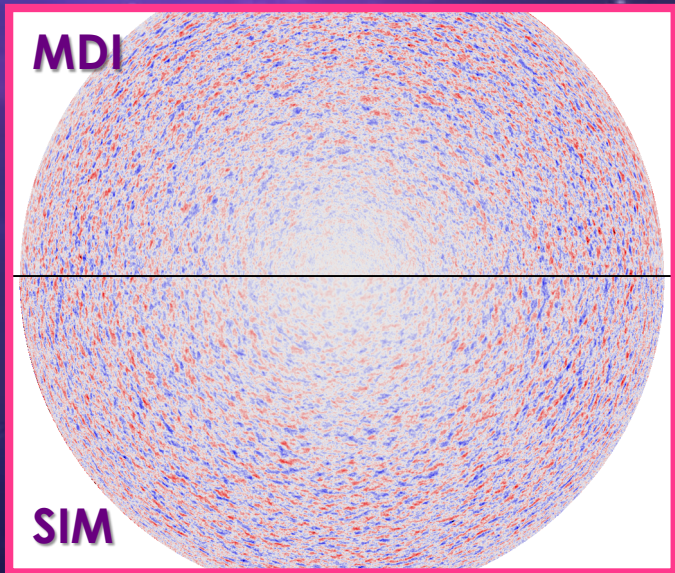
Upton, L., & Hathaway, D. H. 2014a, ApJ, 792, 142  
Upton, L., & Hathaway, D. H. 2014b, ApJ, 780, 5

# Observed Flows

## ☀ Differential Rotation

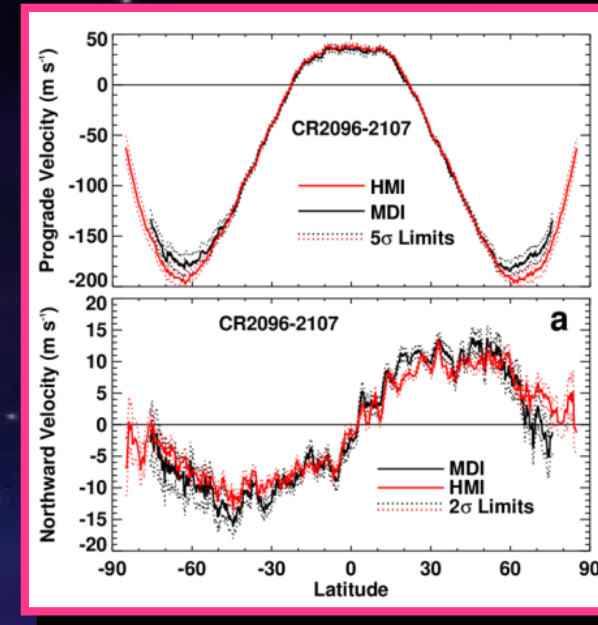
## ☀ Meridional Flow

- Measured with Feature Tracking.
- Averaged over each 27-day rotation.
- Smoothed in time and integrated in the model.



## ☀ Convective Flow

- Explicit convective simulation rather than a diffusivity coefficient alone.
- The convective simulation uses an evolving spectrum of spherical harmonics.
- Reproduces the observed velocity spectrum, the cell lifetimes, and the cell motions in longitude and latitude.



# Source Magnetic Field

AFT can operate under two different regimes: by assimilating magnetograms or by simulating active region emergence.

## Data Assimilation

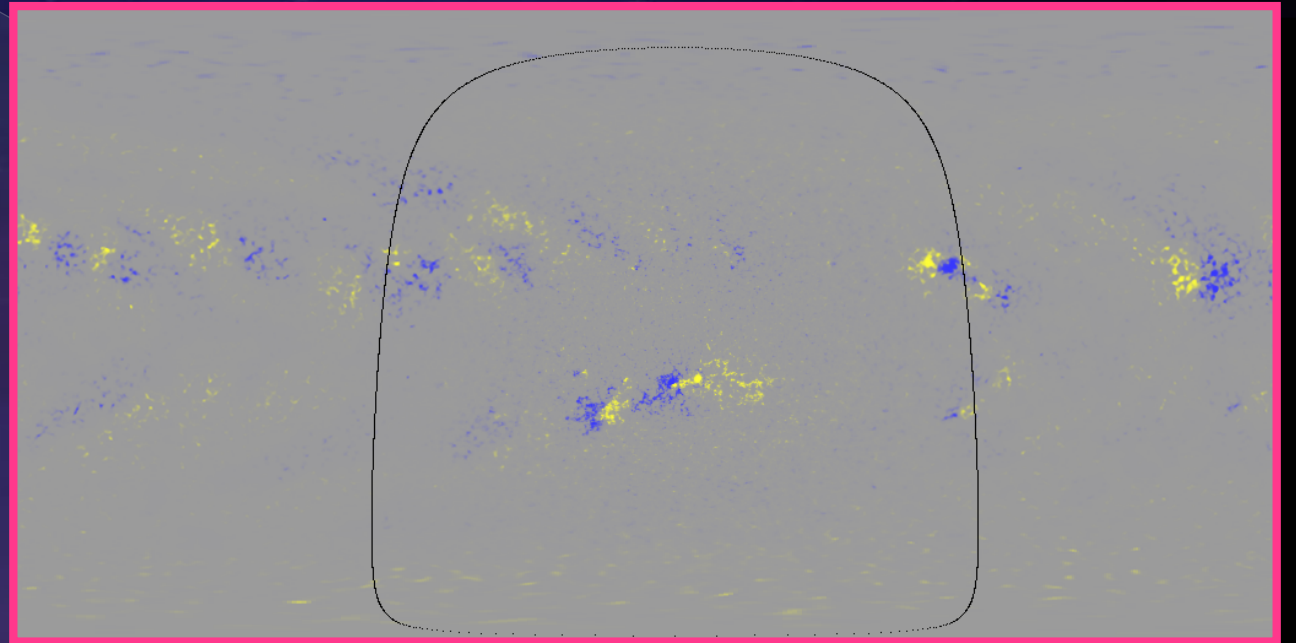
- Corrects for any differences between data and model
- Used to create a *Baseline* for comparisons
- Provides the closest contact with observations

## Simulated Active Regions

- Incorporates active region observations & statistics
- Used for investigating details of flux transport
- Used for *predictive* purposes

# Synchronic Maps

- The AFT model produces magnetic flux maps of the entire Sun with a resolution of 1024 pixels in longitude and 512 pixels in latitude.
- These *synchronic maps* represent the Sun's magnetic field over the entire surface at a moment in time.
- The outlined area contains the magnetic structures as given by magnetograms (SOHO/MDI or SDO/HMI).
- The field outside this area has been transported by our code yet still retains similar network elements and structures.

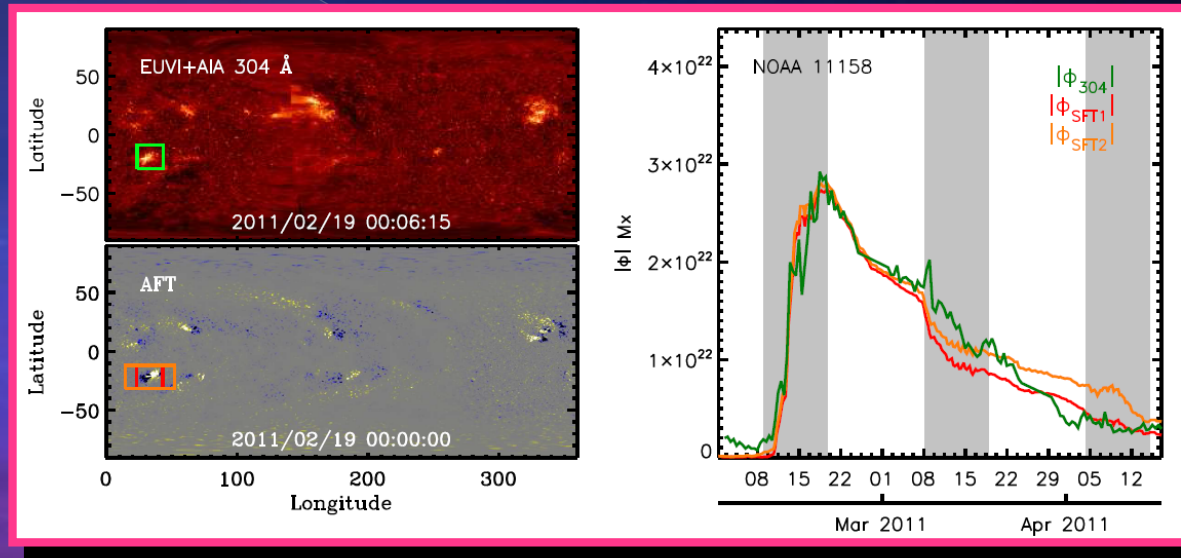


# AFT Movie



Looping video showing 1 year (2015) of AFT

# AFT: Active Region Evolution

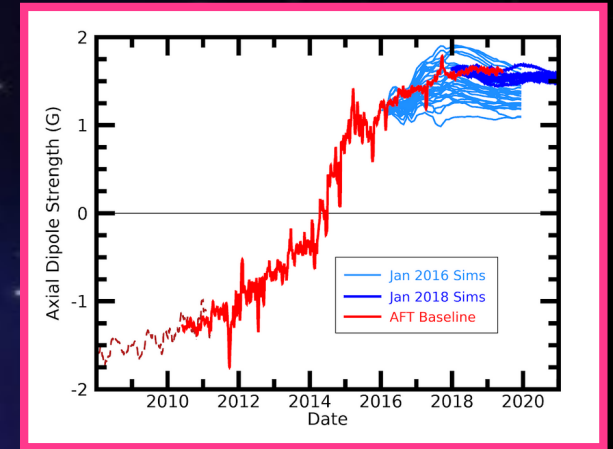
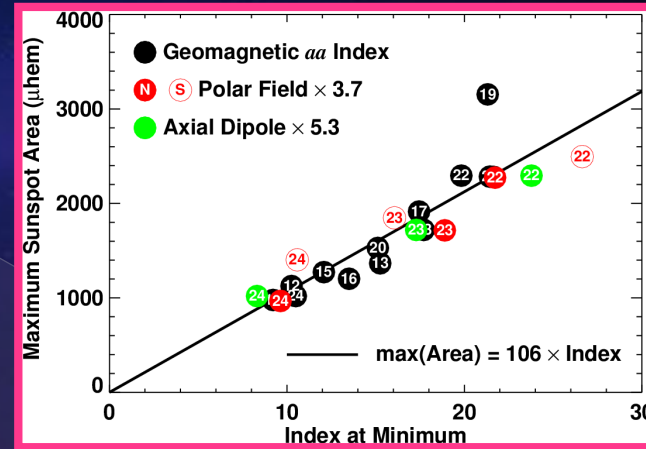
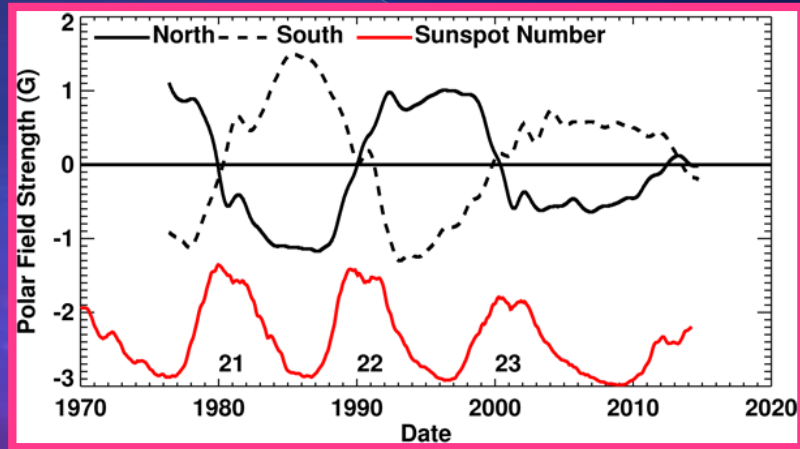


- Work done in collaboration with Harry Warren and Ignacio Ugarte-Urra
- We compared Active Regions in composite EUVI+AIA 304°A and AFT model maps.

- The total unsigned magnetic flux is shown for the 304 Å proxy (green) and for two area integrations of the AFT model (red and orange).
- Grey areas mark the times when the active region is on the Earth side, when data from HMI magnetograms is being assimilated.
- The two are in good agreement for more than two rotations (~60 days) of the AR.



# AFT: Polar Field Evolution



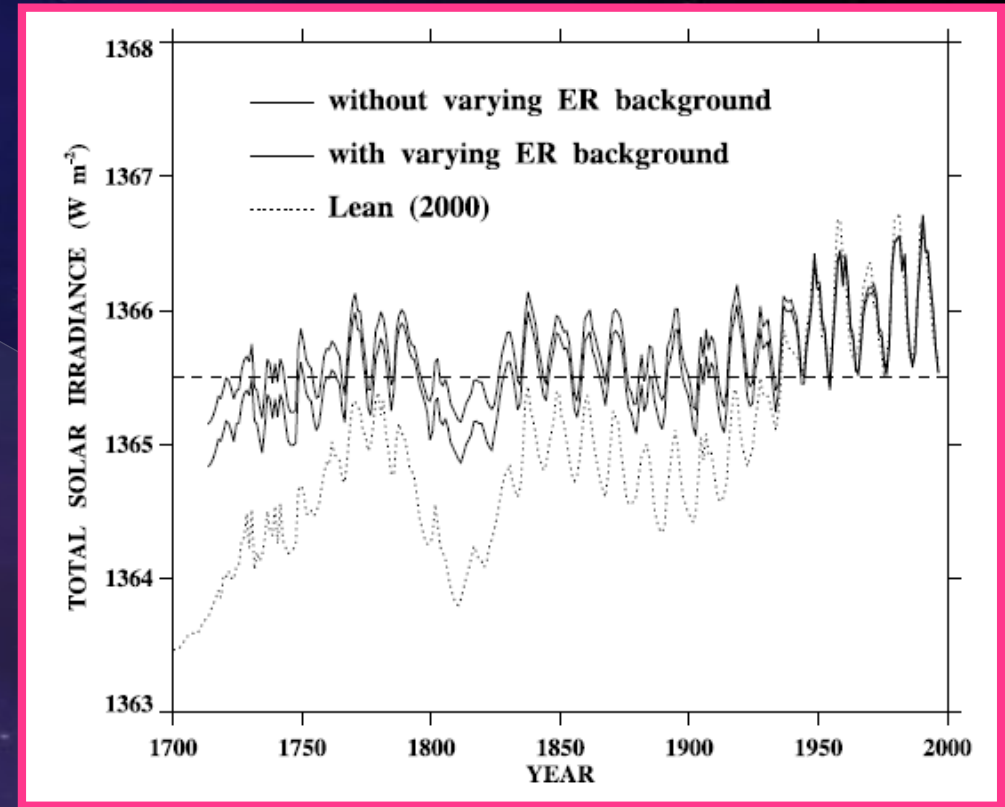
- The strength of the polar magnetic fields at solar cycle minimum have been well established as one of the best predictors of the amplitude of the following cycle.
- AFT has been used to the strength of the evolution of polar fields leading up to the current solar cycle minimum in order to predict the strength of SC 25.
- Observations of the polar fields since then agree with those results.

# Wang, Lean, and Sheeley (2000-2005)

- In the early 2000's, Wang, Lean, and Sheeley used an SFT model to produce a reconstruction of the historical TSI.
- At that time, SFT models were still very young – surface flows and active region properties were poorly constrained.
- In their model, these aspects were highly parameterized:
  - > In order to match the equatorial dipole component, they multiplied the strength of all ARs by a factor of 3.
  - > Two flux emergence algorithms (with a total flux of  $3 \times 10^{25}$  Mx):
    - ❖ Model S1: # of BMRs Scaled according to Cycle Amplitude (each with  $5 \times 10^{22}$  Mx)
    - ❖ Model S2: BMR Strengths Scaled according to Cycle Amplitude (600 total per cycle)
  - > They were unable to reverse the polar field so the Meridional Flow shape and amplitude were tuned.

# Wang, Lean, and Sheeley Results

- They found that the Irradiance is NOT just a function of Open Flux, but rather the Total Flux (Open and Closed)
- They estimated that the increase in TSI between 1713 and 1986 was about 1/2 of its present-day intracycle variation of  $\sim 0.08\%$ .
- They estimated that the cycle-averaged increase in TSI since the Maunder minimum is  $\sim 1 \text{ W/m}^2$ .

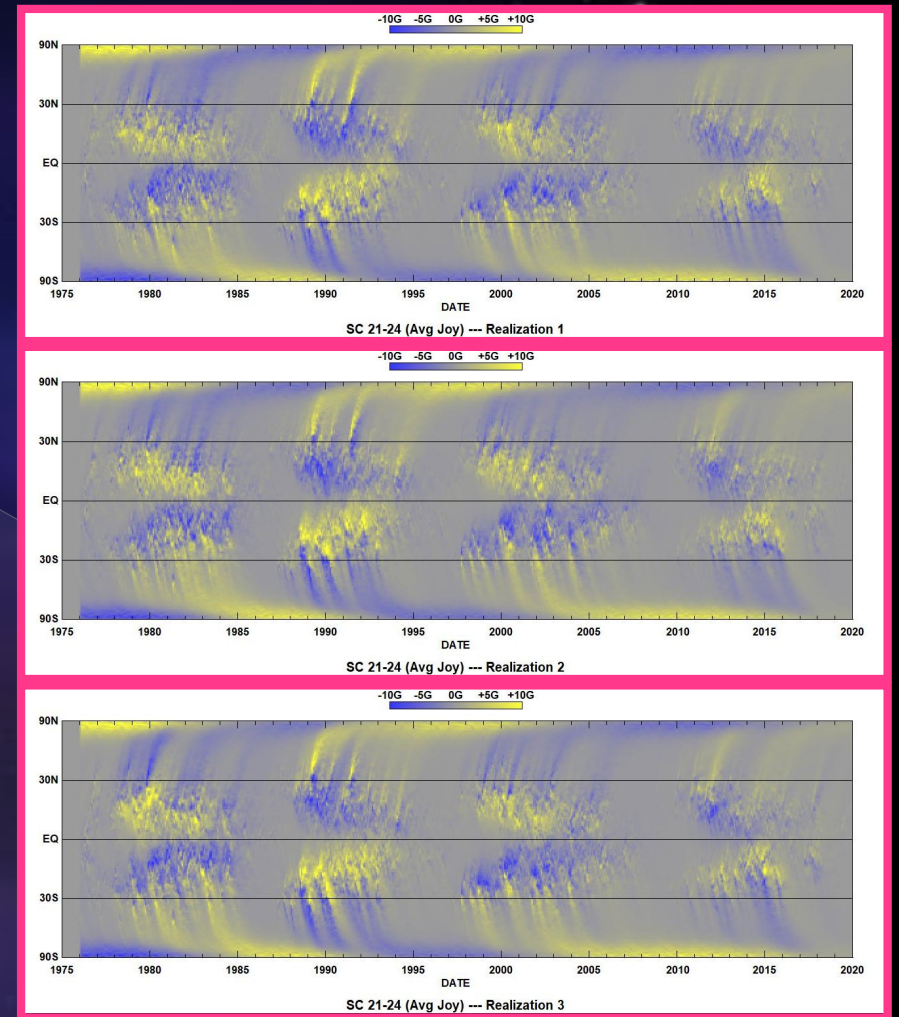


# Nearly two decades later...

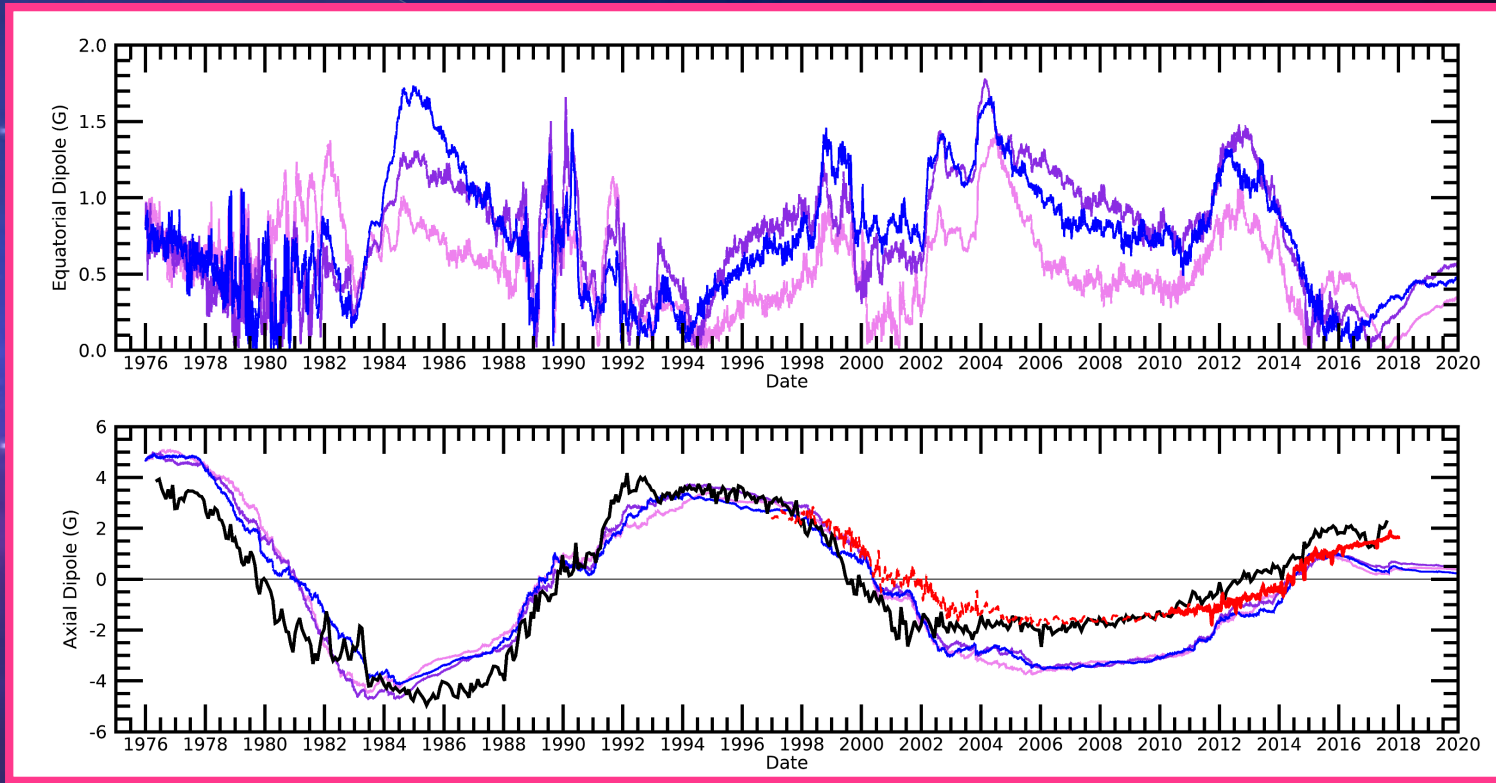
- ◉ We now have revised the SSN (as we just heard from Greg).
- ◉ The Sun's surface flows and active region properties have been significantly constrained.
- ◉ Computational resources are more advanced.
- ◉ We have a new generation of SFT models, such as AFT.

# Modern Cycle Sims – Observed ARs

- The Modern Cycles (21-24) are very well observed.
- Can AFT incorporate the observations and create reversing solar cycles?
  - > Observed Meridional Flow and Differential Rotation.
  - > Active Regions flux and emergence frequency prescribed by the NOAA AR catalog
  - > Average Joy's Tilt and Separation.
- 3 Simulations
  - > Different Convective Realizations



# Simulated Dipole Evolution



- With just 3 realizations (pink, purple, blue), the Equatorial Dipoles varies by a factor of 2.

- Yet the Polar Dipoles remain in good agreement.

- The polar field is in good agreement with the observations (WSO in black and MI/HMI in red) for the first 2 cycles, but diverges during Solar Cycle 23.
- This deviation carried forth into Solar Cycle 24.

# Rogue Active Regions

- According to Jiang et al (2015), “the weak polar fields and thus the weakness of the present cycle 24 are mainly caused by a number of bigger bipolar regions emerging at low latitudes with a “wrong” (i.e., opposite to the majority for this cycle) orientation of their magnetic polarities in the north–south direction, which impaired the growth of the polar field.”
- Nagy et al (2019) found that Rogue ARs, or BMRs with “atypical characteristics can modify the strength of the next cycle via their impact on the buildup of the dipole moment as a sunspot cycle unfolds”, and that

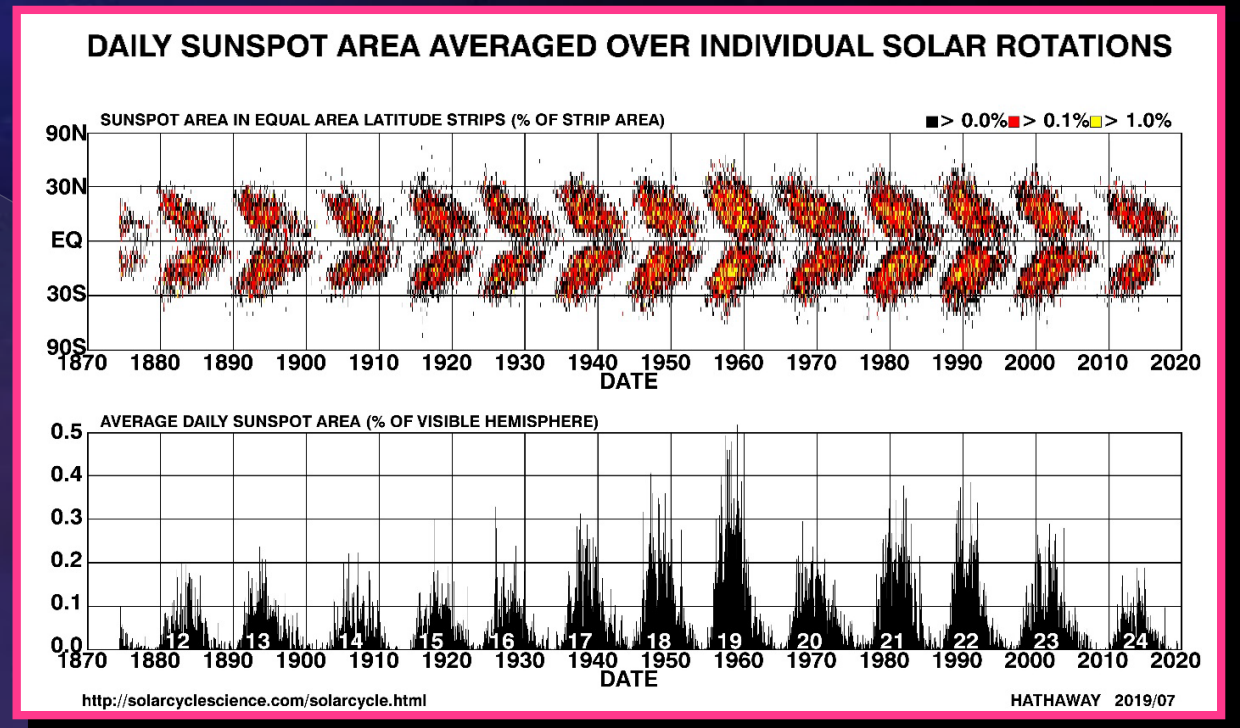
$$\partial \text{Dipole}_{\text{BMR}} = F * d * \sin(\alpha) * \sin(\lambda)$$

where  $F$  is magnetic flux,  $d$  is the angular separation of the two polarities,  $\alpha$  is the tilt angle,  $\lambda$  is the colatitude.

- Since it is essential to get the polar fields correct, we plan to run simulations to investigate using this relationship to introduce Rogue Active Regions into AFT.

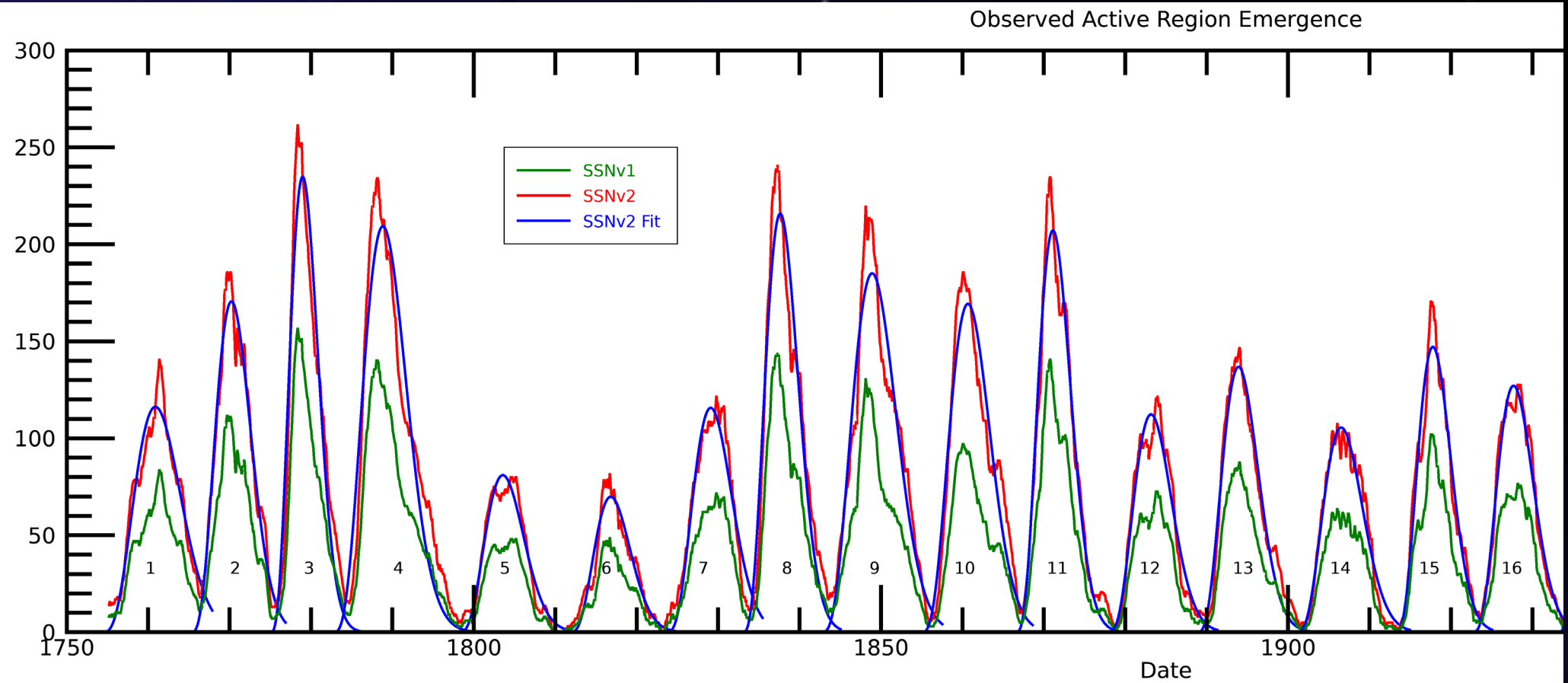
# Synthetic AR Catalogs

- For Historical Solar Cycles (prior to 1874) we do not have detailed AR catalogs.
- We have created an algorithm (based on observed AR Statistics) for generating Synthetic AR catalogs.





# DETERMINING THE TIMING OF EACH CYCLE

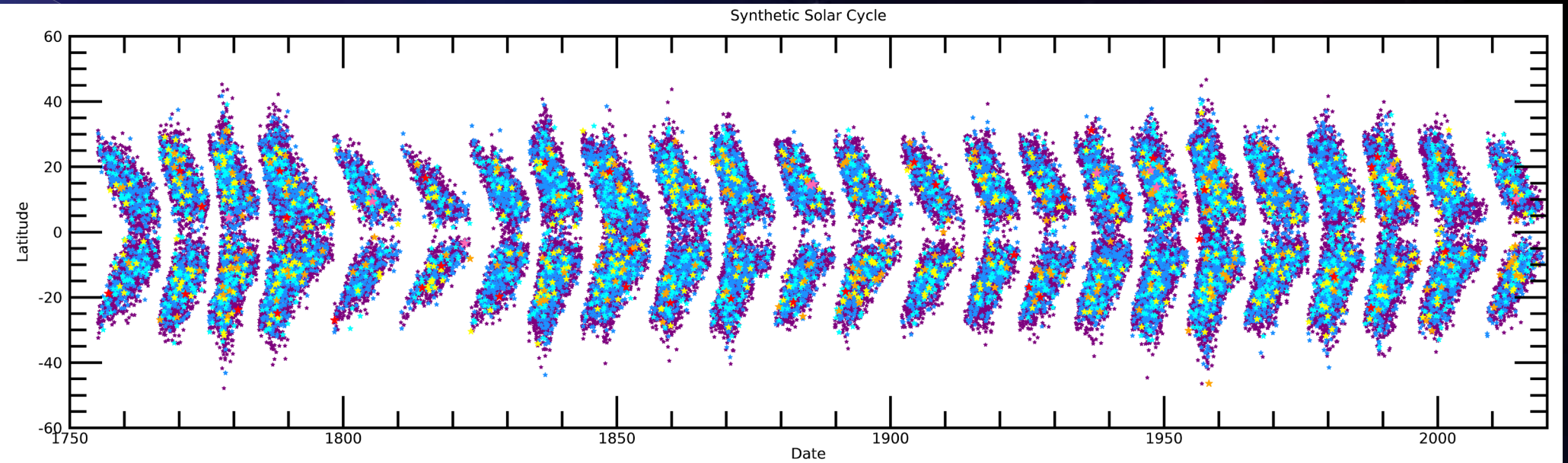


- The monthly Sunspot Number (SSN) is shown for SSNv1 (green) and SSNv2 (red). The fit cycle fits to SSNv2 are also shown (blue).
- We define the Start of the cycle as the time when the blue fits cross the Zero line. Conversely, the End of the cycle is the time of the Start of the next cycle.

# Synthetic Active Regions Properties

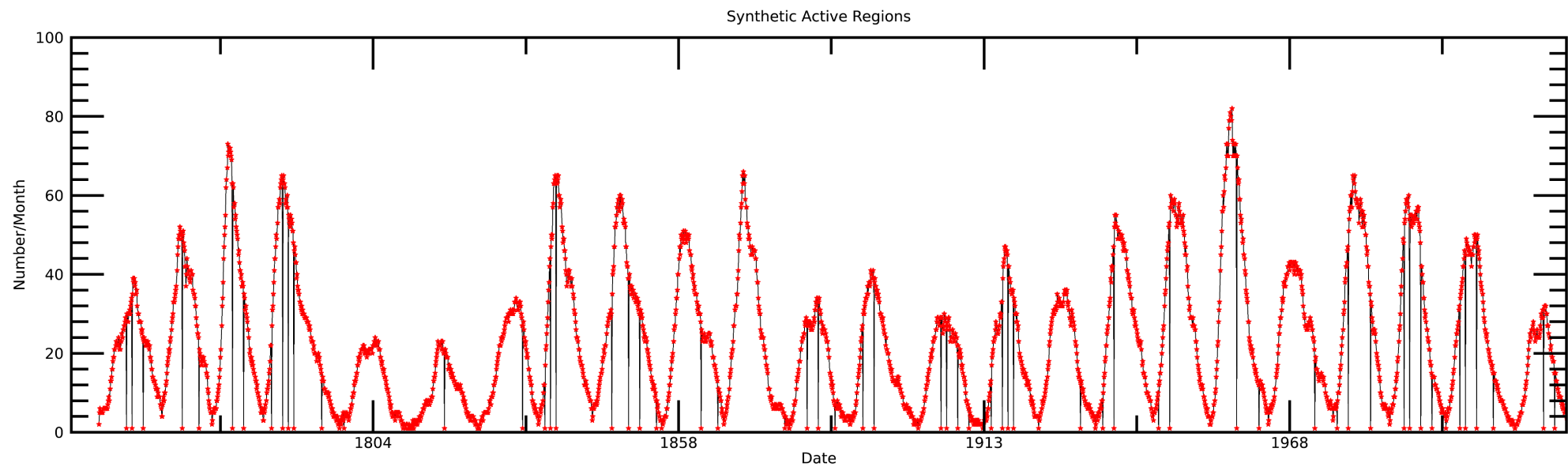
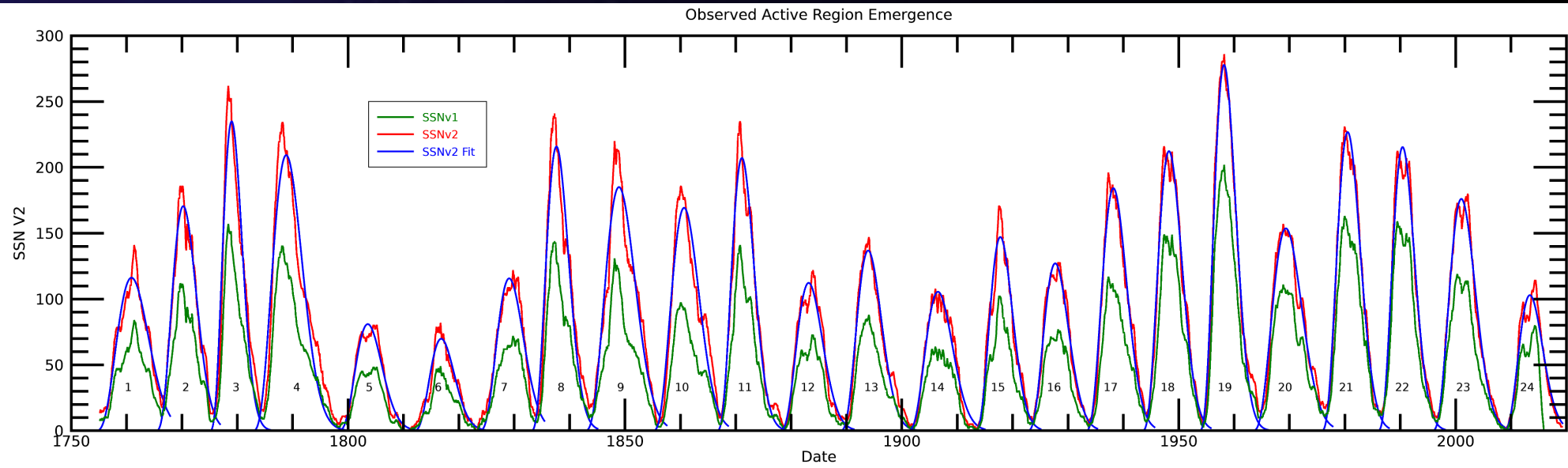
- **Flux** – Based on KPVT/SOLIS BMR Flux distribution (Munjoz-Jaramillo et al, 2016):  $\text{flux} = e^{\mu + \sigma * \delta}$ , where  $\mu = 50.05$ ,  $\sigma = 0.75$ , and  $\delta =$  small deviation (chosen from a Gaussian with a mean of zero and a standard deviation of 1)
- **Area** – where  $\text{Area} = \text{flux} / (7.0 * 10^{19})$  (Sheeley 1966 and Mosher 1977)
- **Hemisphere** is randomly chosen
- **Longitude** randomly chosen
- **Latitude** is determined from the start time of the cycle as (given in Hathaway 2011), where the  $\text{lats} = 28. * e^{-(d\text{months})/90} + d\text{lat}$ , where  $d\text{lat}$  is random variability based on current SSN.
- **Latitude and Longitudinal separation (and tilt angle)** based on Joy's Law and the size and latitude of the Sunspot
- Frequency of Emergence is a function of cycle amplitude (calculated from the NOAA AR catalog) such that the  
**Lag time = (365.24 days/12. month)/[a + b\*(ssn)]**,  $a = 1.33$  &  $b = 0.269$

# SYNTHETIC ACTIVE REGION DATABASE



- The timing, location, and flux for one realization of Synthetic Active Regions for all Solar Cycles 1-24.
- For all 24 cycle, there are a total of 73664 Active Regions with a Flux range of  $2.24e+20$  to  $1.53e+23$  Maxwells
- Flux (and area) are indicated by symbol size and color:
  - Purple/Dark Blue/Aqua:  $1e19$ - $1e22$ / $1e22$ - $2e22$ / $2e22$ - $3e22$  (Mx),
  - Yellow/Orange/Red:  $3e22$ - $4e22$ / $4e22$ - $6e22$ / $6e22$ - $8e22$  (Mx),
  - Pink:  $8e22$  and above

# OBSERVED VERSUS SYNTHETIC



This comparison shows the Observed Sunspot Number (top) and the Number of Newly Emerging Sunspot per month (bottom). While the parameters have different scales, the cycle profiles are well matched.





# Questions and Comments